Geophysical Prospecting, 2008, **56**, 715–727 doi: 10.1111/j.1365-2478.2008.00724.x

Effective permittivity of porous media: a critical analysis of the complex refractive index model

Alessandro Brovelli[1] and Giorgio Cassiani[2]*

[1]*Laboratoire de technologie écologique, Institut des sciences et technologies de l'environnement, École Polytechnique Fédérale de Lausanne, CH-1015 Lausanne, Switzerland, and* [2]*Dipartimento di Geoscienze, Università di Padova, Padova, Italy*

Received October 2006, revision accepted April 2008

ABSTRACT

The availability of reliable constitutive models linking the bulk electric properties of porous media to their inner structure is a key requirement for useful quantitative applications of noninvasive methods. This study focuses on the use of dielectric measurements to monitor fluid saturation changes in porous materials. A number of empirical, semi-empirical and theoretical relationships currently exists that link the bulk dielectric constant with volumetric water content. One such relationship, named complex refractive index model or Lichteneker-Rother model has been extensively applied in recent years. Here we first analyse the characteristics of this Lichteneker-Rother model by means of theoretical considerations. This theoretical analysis indicates that the Lichteneker-Rother exponent is dependent upon the geometrical properties of the porous structure, as well as the permittivity contrast between the different phases. Pore-scale modelling and experimental data further support this result. The parameter estimation robustness in presence of synthetic data error is also assessed. This demonstrates that Lichteneker-Rother parameters cannot, in general, be independently identified on the basis of bulk dielectric constant versus moisture content data.

INTRODUCTION

The development of reliable models for the prediction of effective porous media permittivity is of great importance in geophysics. In recent years, electromagnetic methods, such as ground-penetrating radar (GPR), time-domain reflectometry and electrical resistivity tomography have been adopted for a large number of applications, ranging from, for example, the study of contaminated soils, to hydrogeology and civil engineering (for reviews see Vereecken, Yaramanci and Kemna 2002; Rubin and Hubbard 2005; Butler 2005; Vereecken *et al*. 2005, 2006). The main advantage of such tools is that they allow fast, field-scale and noninvasive surveys. One of the limitations however is the lack of general constitutive relationships that translate the measured data into useful subsurface information, such as moisture content, solute concentration and petrophysical and geotechnical properties of the porous medium.

Most existing models are based on a simple geometry for the porous medium, such as the assumption of grains with a simple, well-defined shape (spherical, ellipsoidal, plate-like, etc.), while a number of other relationships involve some fitting parameters, which are not directly related to the micro-geometrical properties of the medium (Guéguen and Palciauskas 1994; Chelidze and Guéguen 1999; Chelidze, Guéguen and Ruffet 1999; Martinez and Byrnes 2001). With some approximation, three classes of models can be identified: (i) effective medium or mean-field theories, (ii) mixing rules and (iii) empirical relationships.

Mean-field models are derived from Maxwell's studies on effective transport properties of composite media (Maxwell 1891; Wagner 1924) and are based on the physical laws of electromagnetism. Nevertheless, the practical applicability of such models is limited due to their oversimplification of the

*E-mail: giorgio.cassiani@unipd.it

pore structures. Maxwell's approach was further developed, leading to different relationships that have been proved accurate under specific circumstances (Bergman 1978; Sen, Scala and Cohen 1981; Sihvola and Kong 1988, 1989; Robinson and Friedman 2001).

The second class of models introduced above is referred to as 'mixing rules'. These models can be considered as weighted averages of the permittivity of the constituents. A general formula is:

$$\varepsilon_b^\alpha = \sum_{i=1}^{n} \phi_i \varepsilon_i^\alpha \tag{1}$$

where n is the number of porous medium components, the exponent α is a fitting parameter ($-1 \leq \alpha \leq 1$) and ε_b is the bulk permittivity of the medium. Finally, ϕ_i and ε_i are the volume fraction and the permittivity of the i-th phase, respectively. This equation is often named the 'Lichteneker-Rother equation' (Guéguen and Palciauskas 1994). The use of the limiting values is equivalent to replacing the porous medium with an equivalent electrical circuit, with components arranged in series (Fig. 1a) or in parallel (Fig. 1b).

A special model that falls within this class is the well-known complex refractive index model (Birchak *et al.* 1974; Wharton *et al.* 1980; Dobson *et al.* 1985; Heimovaara, Bouten and Verstraten 1994), which is equivalent to equation (1) with $\alpha = 0.5$. Although the complex refractive index model relationship was first derived using an oversimplified description of the porous medium geometry, it produces a good fit in many cases (de Loor 1990; Roth *et al.* 1990; Robinson, Gardner and Cooper 1999; Rubin and Hubbard 2005). A literature review on the Lichteneker-Rother equation and the values assumed by the parameter α under different experimental conditions will be presented in the next section.

The main advantage of the mixing models is their simplicity and the presence of a fitting parameter that helps fitting the experimental data. However, these fitting parameters are not easily related to the properties of the porous medium and its constituents.

Finally, empirical models are expressions obtained by fitting large experimental datasets, with little or no physical significance. The most widely adopted is the Topp, Davis and Annan (1980) model:

$$\varepsilon_b = 3.03 + 9.3\theta + 146\theta^2 - 76.7\theta^3 \tag{2}$$

where θ is the volumetric moisture content [m^3/m^3]. This equation is reported to work reasonably for some typical field conditions (Roth *et al.* 1990). The underlying assumption of the Topp model (equation (2)) is that changes in bulk permittivity are due only to changes in the water content, regardless of the permittivity of the solid constituents and to the internal porous structure. Clearly, such assumptions lead to a certain degree of approximation (West *et al.* 2003). The accuracy and reliability of the Topp equation decrease as the water content decreases, because bulk permittivity is increasingly dominated by the properties of the porous medium solid matrix.

In recent years, several studies have investigated the effect of grain size distribution and particle shape on the bulk permittivity of the medium (Jones and Friedman 2000; Robinson and Friedman 2001; Friedman and Robinson 2002). All these studies concluded that changes of the porous structure have a significant impact that cannot be accounted for by the change in porosity. Nevertheless, neither the complex refractive index model nor the Topp model account for the geometrical properties of the porous structure. Consequently, further work is required to evaluate to what extent the constitutive equations routinely used to predict bulk permittivity of soils are affected by the lack of sensitivity regarding soil microgeometrical properties. In addition, since all the equations used in practical applications need to be calibrated against laboratory data, it is crucial to assess the degree of correlation between the governing parameters and their sensitivity. This latter aspect may have important consequences on model results, as a high degree of correlation between the parameters may reflect negatively on the parameter estimation procedure, thus reducing the accuracy of model predictions.

In this paper we focus on the Lichteneker-Rother equation of which the complex refractive index model is a special case, because it is routinely used and has some theoretical justifications. The first goal of this work is to analyse how the exponent α in the Lichteneker-Rother model varies as a function of different porous medium properties (namely the porosity, the pore geometry and the permittivity of its constituents). The conclusions reached here are used to discuss the complex

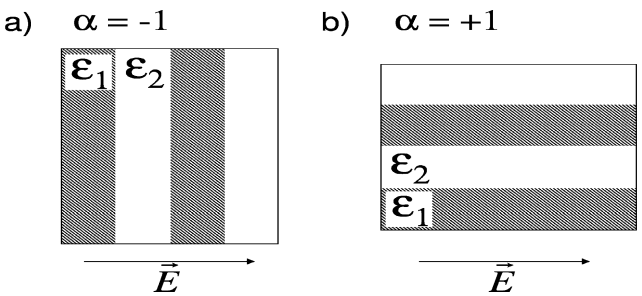

Figure 1 Idealized porous medium with the components arranged as layers: in a) series, b) parallel. The volume fractions are $\phi_1 = \phi_2 = 0.5$.

refractive index model, which assumes a constant value for α. In the second part of the paper we investigate the robustness of the Lichteneker-Rother relationship when the parameter α and the permittivity of the solid matrix ε_s are estimated from a set of experimental data.

THE LICHTENEKER-ROTHER MODEL

For a three-phase system, equation (1) can be written as:

$$\varepsilon_b^\alpha = (1-\phi)\varepsilon_s^\alpha + \theta\varepsilon_w^\alpha + (\phi-\theta)\varepsilon_n^\alpha \tag{3}$$

where ϕ is the porosity, θ the volumetric moisture content, ε_b is the effective (bulk) permittivity of the medium and ε_s, ε_w, ε_n are the permittivities of the solid matrix, the aqueous phase and an immiscible phase (such as air or an organic liquid), respectively.

As already noted, setting $\alpha = 0.5$ reduces equation (3) to the complex refractive index model. Some theoretical proofs of the validity of this latter constitutive relationship have been proposed, which make use of the simplified assumption regarding the distribution of the components within the porous medium (Birchak *et al.* 1974; Zackri *et al.* 1998). For a two-phase medium, assuming that the electromagnetic wave traveltime through the porous medium is equal to the sum of the traveltimes through the separate phases, Birchak *et al.* (1974) recovered equation (3) with $\alpha = 0.5$. This is equivalent to the well-known time-averaged model, frequently used in seismics (Wyllie, Gregory and Gardner 1956). Under the same assumptions, the Lichteneker-Rother model can be further extended to multi-phase porous media.

A self-consistent, effective medium approach was adopted by Zackri *et al.* (1998) to demonstrate that the Lichteneker-Rother equation is physically plausible. Their model computes the equivalent permittivity of a medium composed by a background material, representing the solid matrix, filled with ellipsoidal inclusion. The inclusions can have different volumes and shapes and the inclusion shapes follow a β-distribution. Following their analysis, Zackri *et al.* (1998) concluded that the exponent α is not a constant but varies with the shape of the inclusions and thus with the pore geometry.

Equation (3) has been widely applied in hydrogeophysics to recover useful properties of the subsoil such as porosity and moisture content (e.g., Chan and Knight 1999; Binley *et al.* 2001, 2002; Gloguen *et al.* 2001; West *et al.* 2003). In nearly all practical applications, water and nonaqueous phase liquid permittivities are assumed to be known, while the actual value of matrix permittivity depends on the rock mineralogy and must be estimated, together with the value of α.

Several experimental studies are reported in the literature, which investigate (a) the value of α and (b) how α varies as a function of soil type, mineralogy and fluid phases. For example, Roth *et al.* (1990) calibrated equation (3) on measurements performed in the time-domain reflectometry frequency range and on several soil types with a wide range of clay (2–20%) and organic carbon content. They found $\alpha = 0.46 \pm 0.007$, which is close to the theoretical value of 0.5. Dobson *et al.* (1985) modified the original equation introducing water bound to clay as a fourth phase. In this work, α was found to be 0.65 for soils ranging from sandy loam to silty clay. Other authors have found α to vary in the range 0.25–0.8 both for three-phase systems (solid, water and air) and four-phase systems (solid, water, air and nonaqueous phase liquid) (Jacobsen and Schjonning 1995; Zackri *et al.* 1998; Persson and Berndtsson 2002). Moreover, Persson and Berndtsson (2002) and Ajo-Franklin, Geller and Harris (2004) measured the bulk permittivity of soil samples with variable water, air and nonaqueous phase liquid content (the former used sunflower seed oil as a nonaqueous phase liquid, while the latter used trichloroethylene) and observed a significant dependence of α on the nonaqueous phase liquid volumetric content. In summary, while previous experimental results are somewhat contradictory they indicate that a constant value for α may not be appropriate. This conclusion seems to be further evident for unsaturated porous media. In the following, we will present some considerations on the physical meaning of α, examining in particular its dependence on the solid phase permittivity and porosity.

Dependence of the Lichteneker-Rother exponent α on porous medium geometry

Theoretical considerations

For a two-phase, fully saturated porous medium ($\theta = \phi$), equation (3) reduces to:

$$\varepsilon_b^\alpha = (1-\phi)\,\varepsilon_s^\alpha + \phi\varepsilon_f^\alpha \tag{4}$$

where ε_f is the permittivity of the saturating fluid phase. Dividing both sides of equation (4) by ε_f^α gives:

$$\left(\frac{\varepsilon_b}{\varepsilon_f}\right)^\alpha = (1-\phi)\left(\frac{\varepsilon_s}{\varepsilon_f}\right)^\alpha + \phi \tag{5}$$

We can now evaluate the limit of equation (5) for $\varepsilon_s/\varepsilon_f \to 0$, i.e., the permittivity of the saturating fluid is much larger than

the permittivity of the solid phase. This leads to:

$$\lim_{\varepsilon_s/\varepsilon_f \to 0} \left(\frac{\varepsilon_b}{\varepsilon_f}\right)^{\alpha} = \phi \quad \forall \alpha > 0 \tag{6}$$

which is equivalent to:

$$\left(\frac{\varepsilon_b}{\varepsilon_f}\right)_{\varepsilon_s/\varepsilon_f = 0} = \phi^{\frac{1}{\alpha}} \quad \forall \alpha > 0 \tag{7}$$

Equations (6) and (7) are valid for positive values of α only, because for $\alpha \leq 0$ the limit defined by equation (6) goes to infinity. This restricts our analysis and thus conclusions to the cases where the exponent 'a' is strictly positive, i.e., does not apply in general for the Lichteneker-Rother equation. However, this is only a minor limitation, since all the values of α we found in the literature are positive. Moreover the same conclusions apply to the complex refractive index model because α is set to 0.5.

The dielectric constant in the high-frequency limit, ε and the low-frequency electrical conductivity σ are formally equivalent because of the analogy between the governing equations (Sen *et al.* 1981; Guéguen and Palciauskas 1994):

$$\nabla \cdot (\varepsilon \nabla V) = 0 \tag{8}$$

$$\nabla \cdot (\sigma \nabla V) = 0 \tag{9}$$

This implies that the computation of effective permittivity and of effective electrical conductivity is mathematically equivalent (Sen *et al.* 1981; Guéguen and Palciauskas 1994). As a consequence, although physical processes controlling the displacement and the electrical fluxes are different, the same constitutive equations can be applied, given that the underlying assumptions are honoured. In real systems, electrical conductivity and dielectric constant differ because (i) the contrast in material permittivity is extremely small compared to that of electrical conductivity, (ii) the lowest value for permittivity is 1 (i.e., the permittivity of the air phase), while insulating materials have an electrical conductivity that is in practice negligible (e.g., quartz). Finally, (iii) in natural porous media electrical conductivity is often largely affected by the properties of the water-solid interface (e.g., Brovelli *et al.* 2005). The surface conductivity is mainly attributed to small amounts of conductive materials (clays and oxides) dispersed in the porous medium and to surface charged sites. In the high-frequency limit ion displacement responsible for dielectric loss is not present and consequently the bulk dielectric constant is poorly or non-sensitive to small fractions of clays and oxides.

Under the conditions of insulating porous matrix and negligible surface conductivity ($\sigma_s = 0$), the bulk electrical conductivity σ_b of porous media can be computed using Archie's law (Archie 1942):

$$\sigma_b = \frac{\sigma_w}{F} = \frac{\sigma_w}{\phi^{-m}} \tag{10}$$

where σ_w is electrical conductivity of the pore-water, F is the formation factor and m is Archie's cementation exponent that depends only on the micro-geometrical properties of the porous medium (e.g., grain shape, connectivity and tortuosity of the pore space) (Sen *et al.* 1981; Revil and Cathles 1999). Although Archie's law (equation (10)) was originally developed as a purely empirical equation, several studies showed that it has rigorous theoretical justifications. Among these, Sen *et al.* (1981) applied a differential self-consistent approach to compute the bulk permittivity and electrical conductivity of a simplified yet realistic porous geometry. One of the main advantages of the Sen *et al.* (1981) model is that the geometrical properties of the pore space and solid matrix are clearly defined and the continuity of the fluid phase is ensured. The Sen *et al.* (1981) approach leads to a simple equation for the bulk conductivity of the system, equivalent to Archie's law with a cementation exponent $m = 2/3$. Some later studies, based on a similar approach (e.g., Rubin and Hubbard 2005), demonstrated that the exponent varies as a function of the grain geometry. Pride (1994) derived a constitutive equation equivalent to equation (10) using instead a volume averaging approach. The Pride (1994) model was further extended (e.g., by Revil and Glover 1998), giving additional insights into the physical meaning of the formation factor and it extended Archie's equation to account for surface conductivity effects.

As discussed, due to the analogy between equations (8) and (9), under certain circumstances equation (10) can be adopted for permittivity. The principal limitation for applying Archie's law to compute the bulk dielectric constant is that the permittivity of the solid matrix must be negligible. As already noted, this is physically impossible, as the lowest possible permittivity is that of air. Nevertheless, an equivalent condition is a large contrast between the solid and the saturating fluid permittivities. When this condition is satisfied, it is possible to combine equations (7) and (10), thus obtaining:

$$\frac{\sigma_b}{\sigma_w} = \phi^m = \left(\frac{\varepsilon_b}{\varepsilon_f}\right)_{\varepsilon_f >> \varepsilon_s} \quad \forall m > 0 \tag{11}$$

Rearranging equation (11), it can be shown that, as the ratio $\varepsilon_s/\varepsilon_f \to 0$, $\alpha \to m^{-1}$. According to equation (7), this result holds only when both parameters α and m are positive. While the exponent α could assume negative values, the cementation

factor is always positive. Thus, for a two-phase, fully saturated porous medium, the Lichteneker-Rother exponent can be related to Archie's cementation exponent when the exponent itself is larger than zero. As already pointed out, this condition is in practice always satisfied.

These results show that the exponent α depends only on the porous medium internal geometry when the solid permittivity is small compared to that of the fluid (equation (10)). This situation is in practice not realizable in natural porous media, because the solid matrix often has a permittivity between 5 and 8 and the saturating fluid with a larger permittivity found in natural conditions is water, $\varepsilon_w = 80$. Thus, $\alpha = m^{-1}$ provides an upper limit for the value of the Lichteneker-Rother exponent. Nevertheless, the above discussion implies that in general α is not a constant (e.g., equal to 0.5, as in the complex refractive index model equation) but is a function of the structural properties of the porous medium.

Dependence of the Lichteneker-Rother exponent α on porosity

Sen *et al.* (1981) published a dataset of bulk permittivity values for glass beads as a function of packing porosities. Experimental observations with three saturating fluids are available, including water ($\varepsilon_f = 79.8$), methanol ($\varepsilon_f = 30$) and air ($\varepsilon_f = 1$).

We used these data to investigate the effect of porosity on the exponent α for a two-phase porous system. The exponent values have been computed using the two-phase Lichteneker-Rother equation (equation (4)). Results are shown in Fig. 2 and are relevant to water, methanol and air, respectively. The dots represent the computed α values, while the solid line is the best fit assuming a linear relationship between porosity ϕ and α. We use the slope of such lines to investigate the correlation between the two parameters. For a saturating fluid with a large permittivity (water) the slope of the fitted lines is close to zero and thus the correlation between ϕ and α is extremely weak. As the permittivity of the saturating fluid decreases, the slope of the fitted line significantly increases towards negative values, indicating a negative correlation between the Lichteneker-Rother exponent α and porosity.

A possible explanation is that with a saturating fluid of high permittivity, the asymptotic value at $\varepsilon_s/\varepsilon_f \to 0$ can be reached with small porosity. However, theoretical analysis indicates that the α value for the water-saturated porous medium is always around 0.5 (Birchak *et al.* 1975).

Dependence of the Lichteneker-Rother exponent α on phase permittivities

Pore-scale modelling

Here we address the possible dependence of α on the permittivity of both the solid matrix and the aqueous phase for a two-phase porous system. Brovelli *et al.* (2005) presented a pore-scale modelling approach developed to compute the bulk electrical properties (conductivity and permittivity) of porous media. The model solves numerically the electrical continuity equation within a digital representation of a porous medium. Each digital sample is composed of a solid matrix, an aqueous phase and possibly an immiscible phase (air or nonaqueous phase liquid). Predicted values of both electrical conductivity and dielectric constant were compared against different experimental datasets, showing an excellent agreement. Further details on the approach and model validation can be found in Dalla *et al.* (2004) and Brovelli *et al.* (2005). A major advantage of such a model is that the permittivity of each phase is defined at the microscopic scale and consequently the impact on the macroscale measurements can be readily investigated for the full range of permittivity contrasts.

Since both porosity and water content are known in the digital porous medium, Archie's cementation exponent is easily computed from equation (11), while α is recovered from equation (4). This latter equation must be solved numerically. The bisection method was adopted and the uniqueness of the solution within the range of interest (−1:1) was verified. Positive values of α were always found.

The porous medium consists of a random packing of digital spheres with a prescribed diameter distribution and porosity. The relevant information pertaining to the digital porous medium used here is provided in Table 1. We conducted several numerical experiments using a fluid saturated digital sample (i.e., only two phases are considered, the solid grains and a fluid/gas). The phase permittivities were varied. For the solid phase the range we investigated was 1–10 while the permittivity of the fluid phase was taken between 10 and 80. These synthetic results are reported in Fig. 3 (solid symbols). In this figure the theoretical upper limit for α is also shown (dashed line). This latter value was computed from Archie's cementation factor m, as discussed above (equation (11)). Figure 3 clearly shows that the fitted exponent α is a function of the phase permittivity. The simulated results confirm the theoretical finding in section 'Dependence of Liehteneker-Rother exponent α on porous medium geometry: Theoretical considerations'. The computed values for the exponent

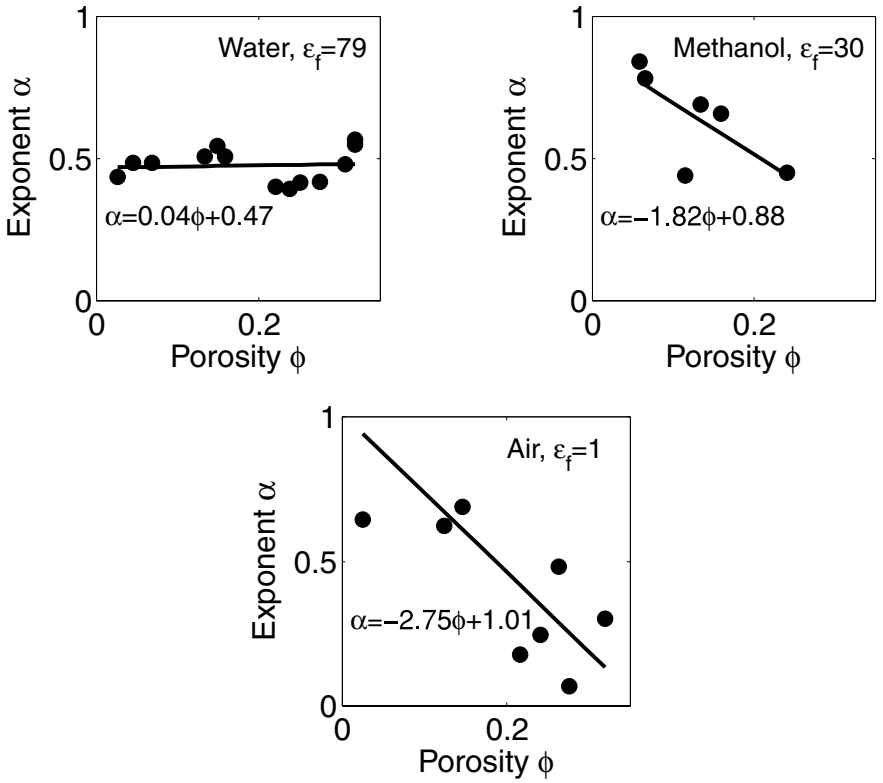

Figure 2 Lichteneker-Rother exponent value as a function of porosity for glass beads (dots). The saturating fluids are water, methanol and air. Experimental data from Sen *et al.* (1981). The solid lines were fitted to identify a possible relationship between the exponent and the porosity.

Table 1 Geometrical and structural properties of the simulated porous medium (based on Brovelli *et al.* 2005)

Property	Value
Grain radius R_g	0.073 ± 0.025 mm
Domain length L	3.987 mm
Porosity ϕ	0.39
Number of spheres	14501
Specific surface area	16.95 mm^{-1}

α approaches m^{-1} as the contrast between the two phases increases.

Comparison with experimental data

Robinson and Friedman (2003) reported extensive permittivity measurements of fluid saturated porous materials. The aim of their study was to develop a method to independently estimate the permittivity of the solid matrix. We use their experimental data to evaluate how the Lichteneker-Rother exponent α varies as a function of the permittivity contrast. While the experimental dataset consists of measurements made on five

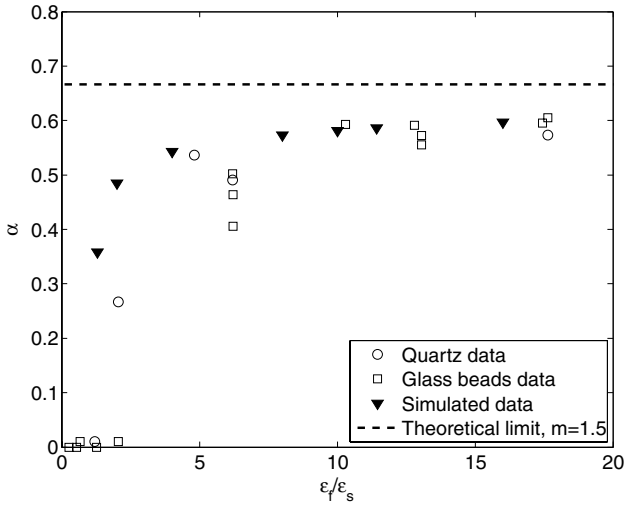

Figure 3 Effect of the permittivity contrast on the Lichteneker-Rother exponent. Pore-scale modelling results from Brovelli *et al.* (2005) and experimental data from Robinson and Friedman (2003).

different porous materials, in this work we only selected measurements performed on glass beads and silica sand, as the remaining materials (seashell fragments, tuff and hematite) are not representative of common geological materials. The

Table 2 Properties of the experimental porous material used (based on Robinson and Friedman 2003)

Property	Glass beads	Silica sand
Grain radius R_g	0.5 mm	0.5 mm
Particle density	2.49 g cm^3	2.65 g cm^3
Porosity ϕ	0.395	0.382
Solid permittivity ε_s	7.6	4.7

relevant properties of the two selected porous media are reported in Table 2. Measurements of bulk permittivity were performed at 25 °C using five different fluids: air ($\varepsilon_f = 1$), penetrating oil ($\varepsilon_f = 2.3$), methylene chloride ($\varepsilon_f = 8.8$), acetone ($\varepsilon_f = 20.8$) and water ($\varepsilon_f = 78.6$). Figure 3 shows the results for glass beads and for silica sand (open symbols), together with the pore-scale modelling results. The theoretical upper limit for α is also indicated. A constant value $m = 1.5$ is used in Fig. 3, because (i) the digital porous medium has a cementation exponent of 1.56, (ii) the value of m for glass beads is around 1.5 (Sen *et al.* 1981) and (iii) clean sands usually have a cementation exponent close to this value (Rubin and Hubbard 2005, Table 4.1).

The relations observed in simulated and experimental data have an analogous shape. As expected, the values of α for the water-saturated silica sands are slightly lower than the corresponding values for glass beads. This is because the corresponding cementation exponent m from the literature is expected to be slightly larger.

Discussion

We conclude that, based on theoretical considerations, α cannot be assumed to be a constant because this parameter depends on both the micro-geometrical properties of the porous medium and the ratio between the matrix and the pore space permittivity. Nevertheless, because water permittivity below 1GHz is close to 80 and the dominant mineralogy of 'geological' porous media is quartz, in most cases a value of $\alpha = 0.5$ seems to be appropriate for fully water-saturated porous media.

In addition, the experimental and simulated data reveal that a relationship possibly exists between α and the matrix permittivity. This is an important finding because typically the matrix permittivity and the complex refractive index model exponent are estimated by performing a (joint) regression analysis on laboratory permittivity data.

LICHTENEKER-ROTHER MODEL PARAMETER ESTIMATION

Following the results obtained above, in this section we focus on the Lichteneker-Rother model parameter estimation and the relevant uncertainty. While some techniques have been developed to estimate the permittivity of the porous medium solid phase, such as that presented in Robinson and Friedman (2003), in daily applications this value is jointly estimated together with the Lichteneker-Rother exponent α. As the findings of section 'The Lichteneker-Rother model' clearly show, some degree of correlation exists between these two parameters, here we develop and apply a procedure to rigorously quantify the degree of correlation. We also investigate if and to what extent the robustness and effectiveness of the regression analysis is affected by the parameter correlation when data are noisy. While the analysis conducted in the previous section is limited to two-phase, fully saturated systems, we now investigate the three-phase Lichteneker-Rother equation, thus taking into account the effect of water saturation.

Methodology

The robustness of the regression and the correlation between the parameters is studied using the method described e.g., in Cassiani *et al.* (1998) and Cassiani, Burbery and Giustiniani (2005). The method consists of the following steps (the superscripts t and e stand for 'true' and 'estimated'):

1 The three-phase Lichteneker-Rother equation (equation (3)) is applied first as a forward model to create a synthetic dataset of bulk permittivity. The parameter pair (α^t, $\varepsilon^t{}_s$) and the porosity ϕ are arbitrarily chosen. The water saturation varies in the range 0.1–1. Water permittivity is assumed equal to 80 and air permittivity is 1.

2 The Gaussian random error is added to the bulk permittivity dataset. Different error levels are investigated from 0% (no error) to 10% error.

3 An estimated parameter set (α^e, $\varepsilon^e{}_s$) is obtained via the least-square regression analysis by fitting the Lichteneker-Rother model to the synthetic, error affected dataset generated in steps 1 and 2. The Nelder-Mead simplex method (Lagarias *et al.* 1998) is used, as implemented in MATLAB.

4 The sum-of-squared-errors function is mapped in the parameter space.

5 Following Draper and Smith (1998), under the assumption of independent Gaussian errors in the data, an approximate

$100(1-\beta)\%$ confidence contour is computed as:

$$S(\alpha, \varepsilon_s) = S(\alpha^e, \varepsilon_s^e)\left\{1 + \frac{2}{n-2}F(2, n-2, 1-\beta)\right\} \quad (12)$$

where β is the confidence level, chosen arbitrarily as 0.05 for this study. S is the sum-of- squares-error objective function, n is the number of observation points (number of data in the synthetic dataset, i.e., number of different saturation values) and $F(.)$ is the Fisher distribution function. Note that the joint (α, ε_s) confidence region computed by using equation (12) is exact in shape but only approximate in the confidence level because the Lichteneker-Rother model is non-linear.

The bulk permittivity of a porous medium is strongly affected not only by matrix permittivity and the exponent α but also by porosity and fluid permittivity (see previous section). While the latter can be assumed constant for water and air, the former has a relatively broad range of variability. As a result the effect of porosity was also examined.

Indices for the sensitivity study

Following Cassiani *et al.* (2005), we computed a set of indices to provide a brief and quantitative description of the results. Figure 4 shows the 'geometrical' meaning of the indices described below.

To assess the robustness of the studied model, we computed the normalized parameters $\alpha' = \alpha^e/\alpha^t$ and $\varepsilon_s{}' = \varepsilon_s{}^e/\varepsilon_s{}^t$. These values are related to the percent error introduced by the regression analysis, $(1 - \alpha')* 100$ and $(1 - \upsilon))*100$.

The correlation between the two parameters is evaluated from the slope s of a linear regression fit to the confidence region mapped in the parameter space. A value of $|s| = 1$ indicates perfect correlation, while as $|s| \to 0$ or $|s| \to \infty$ the parameters become completely independent. Additionally, the sensitivity of each parameter was evaluated from the relative sizes of the (nearly elliptical) confidence region, $\Delta\alpha' = (\alpha_{max}{}' - \alpha_{min}{}')$ and $\Delta\varepsilon_s{}' = (\varepsilon_{s(max)}{}' - \varepsilon_{s(min)}{}')$. The subscript 'min' and 'max' refer to the upper and lower limit of the confidence interval for each parameter. Because the size of the confidence region is related to the error level adopted, the sensitivity measure adopted also incorporates the effect of noise. Note that the sensitivity index used in this work decreases as the sensitivity increases: for a given error level the smaller the sensitivity the broader the confidence region.

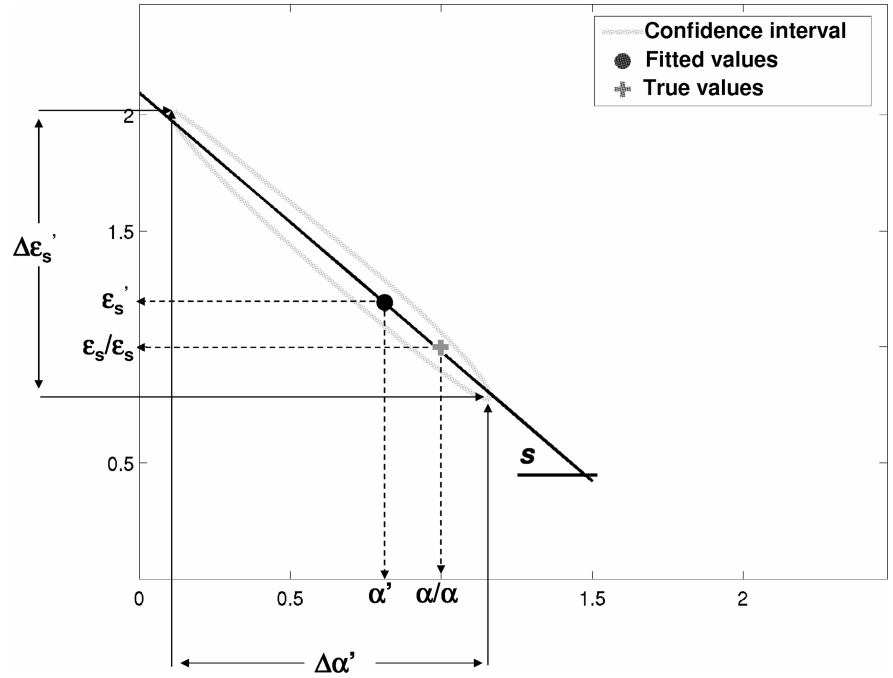

Figure 4 Indices used in the Lichteneker-Rother sensitivity and regression robustness analysis. The closed dot is the normalized true value (i.e., the value used to create the synthetic dataset), the cross corresponds to the values estimated via regression analysis and normalized. The solid line represents the contour of the 0.95 confidence interval for the estimate.

Results

Figure 5 shows four examples of the sensitivity analysis results. Two porosities (0.35 and 0.25) and two values of matrix permittivity (5.0 and 6.5) are investigated. These values were selected as they are in the typical range for sands: clean sands have a matrix permittivity of about 5.0, while the dielectric constant of sands/sandstones with a moderate clay content is usually found in the range 6–6.5 (Guéguen and Palciauskas 1994). In this first set of simulations, the Lichteneker-Rother exponent α is kept constant and equal to 0.5 (i.e., the value derived from theoretical considerations) and the random error added to the dataset is 5%.

The water saturation range for the forward model is 0.1–1, divided into 10 steps. As a result the water saturation / bulk permittivity relationship consists of 11 values. The robustness and accuracy of the regression may be influenced by the data density. The value we adopted is fully consistent with laboratory measurement techniques.

Figure 5 demonstrates that a high degree of correlation exists between the matrix permittivity and the Lichteneker-Rother exponent α, as the 95% confidence levels are an elongated region of nearly elliptical shape. Moreover, repeated numerical experiments indicate that even with a relatively small data error, the estimated values may fall outside the 95% confidence region (not shown in Fig. 5). Results for the error level of 0% are not reported as the computed confidence level was always lower than 10^{-6}. Results obtained using a larger error (10%) are also not reported as they show the same behaviour as the case with a 5% error but with larger values of the indices.

Following these considerations, we studied the indices ($\alpha\prime$, $\varepsilon_s\prime$, s, $\Delta\alpha\prime$, $\Delta\varepsilon_s\prime$) described in the previous paragraph for the porosity range $\phi = 0.1$–0.4. This porosity range can be considered representative of natural porous media. For each given combination of porosity, matrix permittivity and exponent α, 50 different datasets of bulk permittivity versus volumetric moisture content have been generated by adding random Gaussian noise of the prescribed error level (e.g., 5%). For each dataset the estimated values (α^e, $\varepsilon_s{}^e$), the confidence region and the indices were calculated. Finally, the mean value and the standard deviation of each index over the 50 relevant realizations were computed. The results are shown in Figs 6–10. Four different pairs of parameter values for (α^r,

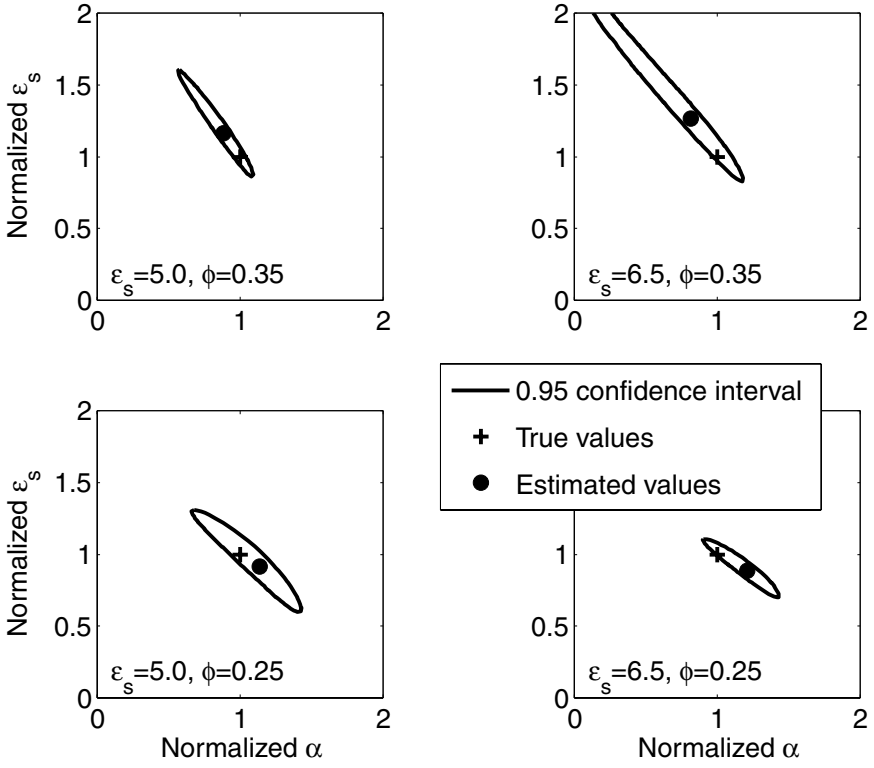

Figure 5 Lichteneker-Rother inverse problem robustness. Examples showing the shape and size of the confidence interval for different values of porosity and matrix permittivity.

ε_s^r) were adopted: (0.5, 5.0), (0.65, 6.5), (0.65, 5.0) and (0.5, 6.5). As discussed above, the matrix permittivity values selected were within the natural range for sand. The value of $\alpha = 0.5$ was also chosen as a 'typical' value for natural porous media, while $\alpha = 0.65$ is the value computed in section 'The Lichteneker-Rother model' for the $\varepsilon_s/\varepsilon_f \to 0$ limit.

Figure 6 reports the mean error for the estimated Lichteneker-Rother exponent (left panel) and matrix permittivity (right panel). The mean error of both parameters is constant and low for all four cases. The error however is slightly larger for the matrix permittivity than for the exponent. In Figure 7 we show the standard deviation of the error. The standard deviation of α decreases slightly over the porosity range but the level is different for the four cases considered. The standard deviation of matrix permittivity steadily increases with porosity from 0.05 to roughly 0.1 (Fig. 7). As previously pointed out in the section 'Indices for the sensitivity study', the normalized parameters used here (1 – mean value and standard deviation) are actually a percent error on the estimates. We can conclude that the mean error remains within the 5% error, which is the random error added to the synthetic dataset but the error of a single estimate often falls outside this value.

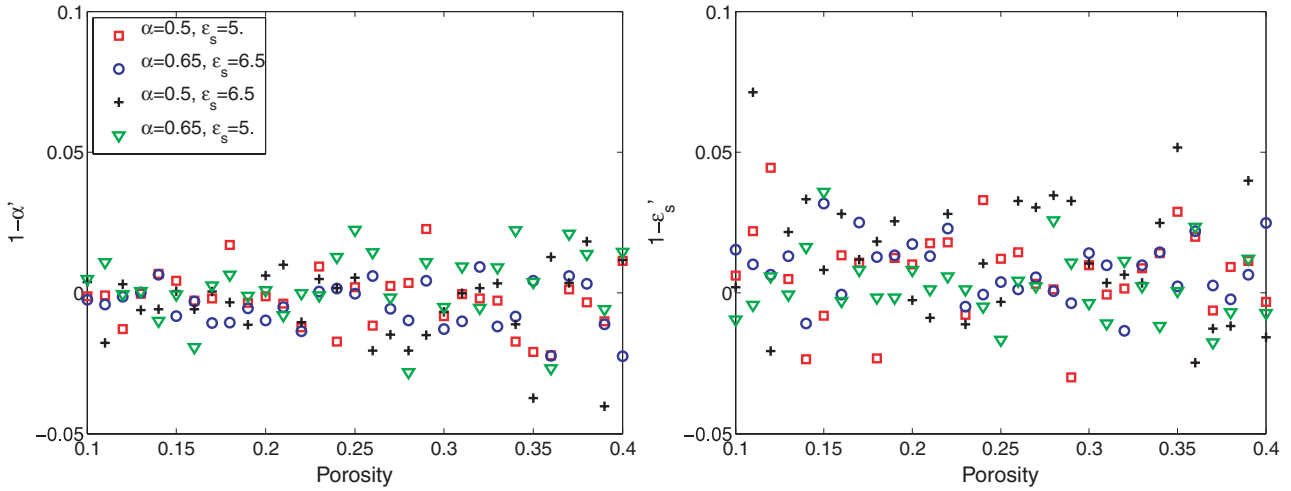

Figure 6 Mean error between the true value and the parameters estimated by regression analysis. No correlation between the two indexes and the porosity is observable for both the parameters.

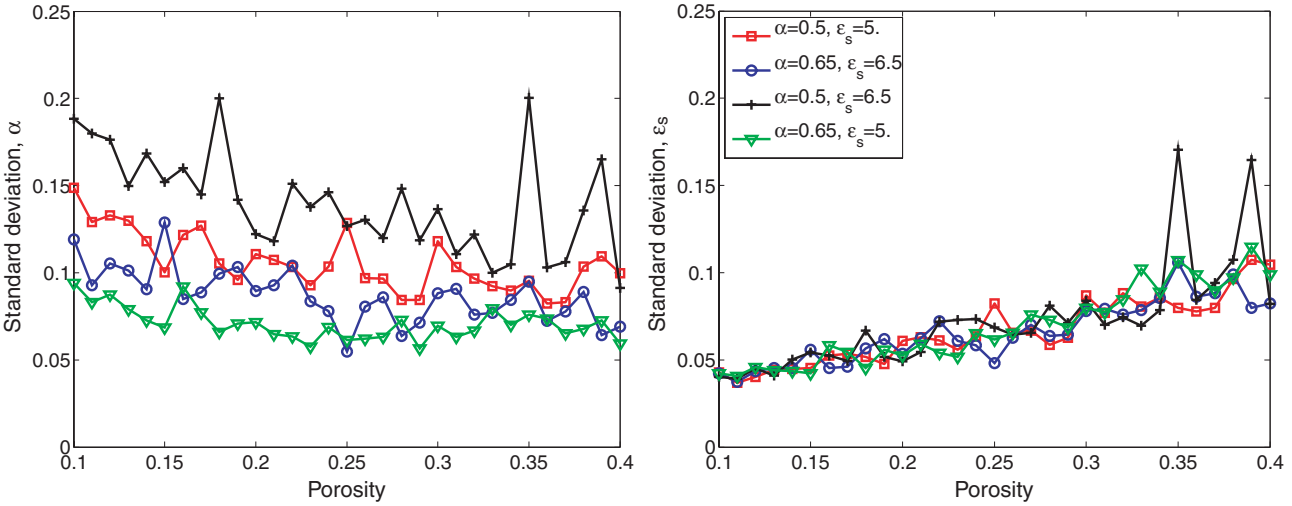

Figure 7 Standard deviation of the error between the estimated and true values. The large values of standard deviation observed indicate that the estimated values can easily fall outside the 95% confidence region, thus resulting in a poor model calibration and non accurate parameter estimation.

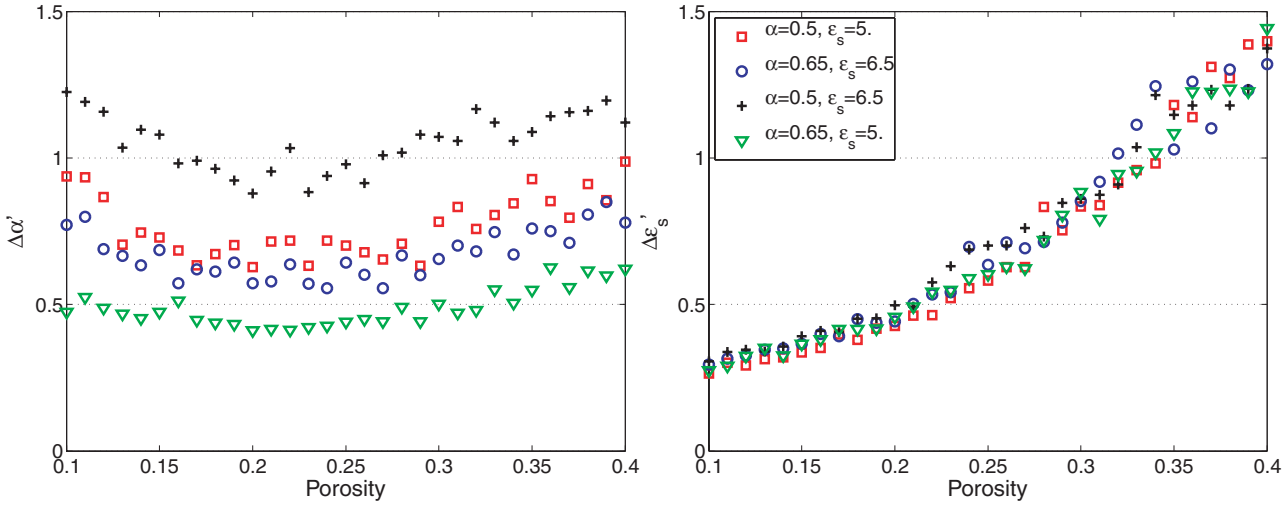

Figure 8 Inverse problem robustness. Relative dimensions of the confidence contour. This parameter provides information on the relative sensitivity of each parameter, with larger values indicating a lower sensitivity.

The relative sensitivity of the two parameters is reported in Fig. 8. The sensitivity of α remains relatively constant over the porosity range. However, the four studied cases show a different behaviour and no clear dependence of sensitivity on 'true' model parameter values can be identified. On the contrary, the relative sensitivity of ε_s steadily decreases as the porosity increases and the studied parameter sets show similar behaviour (Fig. 8). Note that the parameter sensitivities reflect the behaviour observed in the standard deviation of the normalized error. Figure 9 shows the parameter correlation for the four cases. The correlation varies as a function of porosity, matrix permittivity and exponent value. It can also be seen that all four cases have a porosity where the correlation is perfect (i.e., the correlation index $|s| = 1$).

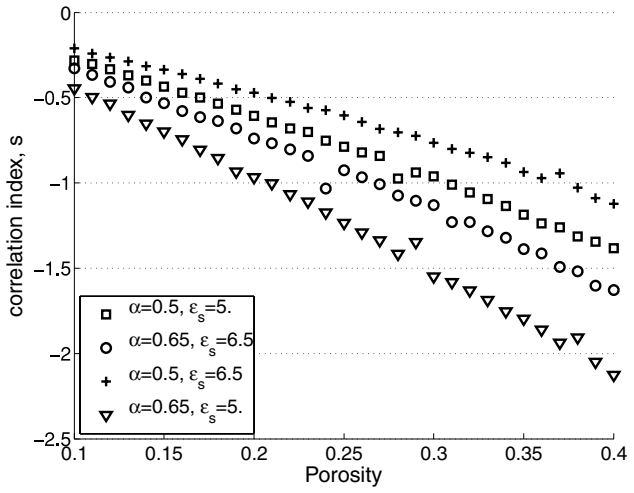

Figure 9 Investigation of the parameter correlation as a function of porosity. A value of –1 indicates a complete inverse correlation of the two properties. All four parameter pairs show a high degree of correlation, which may result in poor parameter estimation.

DISCUSSION AND CONCLUSIONS

In this paper we analysed the characteristics of a classical mixing model for the bulk permittivity of multiphase media – the Lichteneker-Rother model (often referred to as complex refractive index model when the Lichteneker-Rother exponent $\alpha = 0.5$). From this analysis some general conclusions could be drawn:

1 The exponent α (for $\alpha > 0$) is linked to Archie's cementation exponent m and is consequently a function of the geometrical properties of the porous medium. We also found that the exponent α depends on the ratio between the matrix and fluid phase permittivities, i.e., the relative permittivity of the fluid phase compared to that of the solid matrix (paragraph 2.2).

2 The two key Lichteneker-Rother parameters (α, ε_s) are inversely correlated. This results from the shape of the confidence interval, which is an elongated ellipsoid with the axis not parallel to the (α, ε_s) axes.

3 The parameter estimates are unbiased (correct on average) but due to large parameter correlation, the extent of the confidence region may be very large. As a result, the error affecting a single estimation may be substantial. This may have important practical consequences on the accuracy of parameter estimation from field and laboratory measurements.

We conclude that the Lichteneker-Rother model is not entirely satisfactory either in terms of parameter meaning or as a purely empirical tool to represent laboratory data. Future research will involve the development of an alternative constitutive model that should (a) be physically based and (b) involve only parameters that can be easily measured independently and not only fitted to the dielectric response of a sample. The physical basis of such a model could rest upon the Hashin and Shtrikman (1962) lower and upper bounds for bulk permittivity.

ACKNOWLEDGEMENTS

This work was partly supported by the Consorzio Interuniversitario CINECA and by the Italian Ministry of Education, University and Research (MIUR) FIRB grant RBAU01TAL5 'Spectral Induced Polarization for the identification of organic pollutants in the subsurface' and the (MIUR) COFIN grant 2005043992 'Study, definition and analysis of constitutive models linking the DC and induced polarization electrical response to the physical and chemical microstructure of multiphase porous media'. The authors would like to acknowledge D.A. Robinson for providing some of the experimental datasets.

REFERENCES

Ajo-Franklin J.B., Geller J.T. and Harris J.M. 2004. The dielectric properties of granular media saturated with DNAPL/water mixtures. *Geophysical Research Letters* **31**, L17501.

Ansoult M.L., De Baker W. and Declercq M. 1985. Statistical relationship between apparent dielectric constant and water content in porous media. *Soil Science Society of America Journal* **49**, 47–50.

Archie G.E. 1942. The electrical resistivity log as an aid in determining some reservoir characteristics. *Transactions American Institute Mining Metallurgical and Petroleum Engineers* **146**, 54–62.

Bergman D.J. 1978. The dielectric constant of a composite material. A problem in classical physics. *Physics Reports (section C of Physics Letter)* **43**, 377–407.

Berryman J.G. 1992. Effective stress for transport properties of inhomogeneous porous rocks. *Journal of Geophysical Research* **97**, 17409–17424.

Binley A., Cassiani G., Middleton R. and Winship P. 2002. Vadose zone model parameterisation using cross-borehole radar and resistivity imaging. *Journal of Hydrology* **267**, 147–159.

Binley A., Winship P., Middleton R., Pokar M. and West J. 2001. High resolution characterization of vadose zone dynamics using cross-borehole radar. *Water Resources Research* **37**, 2639–2652.

Birchak J.R., Gardner C.G., Hipp J.E. and Victor J.M. 1974. High dielectric constant microwave probes for sensing soil moisture. *Proceedings of the IEEE* **62**, 93–98.

Brovelli A., Cassiani G., Dalla E., Bergamini F. and Pitea D. 2005. Electrical properties of partially saturated sandstones: Novel computational approach with hydrogeophysical applications. *Water Resources Research* **41**, W08411. doi:10.1029/2004WR003628.

Butler D.K. 2005. Near-Surface Geophysics. *Investigations in Geophysics* **13**. SEG.

Cassiani G., Bohm G., Vesnaver A. and Nicolich R. 1998. A Geostatistical framework for incorporating seismic tomography auxiliary data into hydraulic conductivity. *Journal of Hydrology* **206**, 58–74.

Cassiani G., Burbery L.F. and Giustiniani M. 2005. A note on *in situ* estimates of sorption using push-pull tests. *Water Resources Research* **41**, W03005. doi:10.1029/2004WR003382.

Chan C.Y. and Knight R. 1999. Determining water content and of saturation from dielectric measurements in layered materials. *Water Resources Research* **35**, 85–93.

Chelidze T.L. and Guéguen Y. 1999a. Electrical spectroscopy of porous rocks: A review. I. Theoretical models. *Geophysical Journal International* **137**, 1–15.

Chelidze T.L., Guéguen Y. and Ruffet C. 1999b. Electrical spectroscopy of porous rocks: A review. II. Experimental results and interpretation. *Geophysical Journal International* **137**, 16–34.

Dalla E., Cassiani G., Brovelli A. and Pitea D. 2004. Electrical conductivity of unsaturated porous media: Pore-scale model and comparison with laboratory data. *Geophysical Research Letters* **31**, L05609. doi:10.1029/2003GL019170.

De Loor G.P. 1990. The dielectric properties of wet soils. BCRS Report No. 90-13 Proj. No. AO-2.1. The Netherlands Remote Sensing Board, Delft, The Netherlands.

Dobson M.C., Ulaby F.T., Hallikainen M.T. and El-Rayes M.A. 1985. Microwave dielectric behaviour of wet soils, II Dielectric mixing models. *IEEE Transactions on Geoscience and Remote Sensing* **GE-23**, 35–46.

Draper N.R. and Smith H. 1998. *Applied Regression Analysis*, 3rd edn. John Wiley.

Friedman S.P. 1997. Statistical mixing model for the apparent dielectric constant of unsaturated porous media. *Soil Science Society of America Journal* **61**, 742–745.

Friedman S.P. and Robinson D.A. 2002. Particle shape characterization using angle of repose measurements for predicting the effective permittivity and electrical conductivity of saturated media. *Water Resources Research* **38**, 1236. doi:10.1029/2001WR000746.

Gloguen E., Chouteau M., Marcotte D. and Chapuis R. 2001. Estimation of hydraulic conductivity of an unconfined aquifer using cokriging of GPR and hydrostratigraphic data. *Journal of Applied Geophysics* **47**, 135–152.

Glover P.W.J., Hole M.J. and Pous J. 2000. A modified Archie's law for two conducting phases. *Earth and Planetary Science and Letters* **180**, 369–383.

Guéguen Y. and Palciauskas V. 1994. *Introduction to the Physics of Rocks*. Princeton University Press.

Hashin Z. and Shtrikman S. 1962. A variational approach to the theory of the effective magnetic permeability of multiphase materials. *Journal of Applied Physics* **33**, 3125–3131.

Heimovaara T.J., Bouten W. and Verstraten J.M. 1994. Frequency domain analysis of time-domain reflectometry waveforms. 2. A

four component complex dielectric mixing model for soils. *Water Resources Research* **30**, 201–209.

Jacobsen O.H. and Schjonning P. 1995. Comparison of time-domain reflectometry calibration function for soil water determination. *Proceedings of the Symposium: Time-Domain Reflectometry Applications in Soil Science*, pp. 25–33.

Jones S.B. and Friedman S.P. 2000. Particle shape effects on the effective permittivity of anisotropic or isotropic media consisting of aligned or randomly oriented ellipsoidal particles. *Water Resources Research* **36**, 2821–2833.

Lagarias J.C., Reeds J.A., Wright M.H. and Wright P.E. 1998. Convergence properties of the Nelder-Mead Simplex Method in Low Dimensions. *SIAM Journal of Optimization* **9**, 112–147.

Martinez A. and Byrnes A.P. 2001. Modeling dielectric-constant values of geologic materials: An aid to ground penetrating radar data collection and interpretation. *Current Research in Earth Sciences* **247**.

Maxwell J.C. 1891. *A Treatise on Eelectricity and Magnetism*. Dover Publishing. Inc., New York

Persson M. and Berndtsson R. 2002. Measuring nonaqueous phase liquid saturation in sil using time-domain reflectometry. *Water Resources Research* **38**, 1064. doi:10.1029/2001WR000523.

Pride S. 1994. Governing equation for the coupled electromagnetics and acoustics of porous media. *Physical Review B* **50**, 15678–15696.

Revil A. and Cathles III L.M. 1999. Permeability of shaly sands. *Water Resources Research* **35**, 651–662.

Revil A. and Glover P.W.J. 1998. Nature of surface electrical conductivity in natural sands, sandstones and clays. *Geophysical Research Letters* **25**, 691–694.

Robinson D.A. and Friedman S.P. 2001. Effect of particle size distribution on the effective dielectric permittivity of saturated granular media. *Water Resources Research* **37**, 33–40.

Robinson D.A. and Friedman S.P. 2003. A method for measuring the solid particle permittivity or electrical conductivity of rocks, sediments and granular materials. *Journal of Geophysical Research* **108**, 2076. doi:10.1029/2001JB000691.

Robinson D.A., Gardner C.M.K. and Cooper J.D. 1999. Measurement of relative permittivity in sandy soils using TDR, capacitance and theta probes: Comparison, including the effects of bulk soil electrical conductivity. *Journal of Hydrology* **223**, 198–211.

Roth K., Schulin R., Fluher H. and Attinger W. 1990. Calibration of time-domain reflectometry for water content measurement using a composite dielectric approach. *Water Resources Research* **26**, 2267–2273.

Rubin Y. and Hubbard S.S. 2005. *Hydrogeophysics*. Springer.

Sen P.N., Scala C. and Cohen M.H. 1981. A self-similar model for sedimentary rocks with application to the dielectric constant of fused glass beads. *Geophysics* **46**, 781–795.

Sihvola A. and Kong J.A. 1988. Effective permittivity of dielectric mixtures. *IEEE Transactions on Geoscience and Remote Sensing* **26**, 420–429.

Sihvola A. and Kong J.A. 1989. Correction to 'Effective permittivity of dielectric mixtures'. *IEEE Transactions on Geoscience and Remote Sensing* **21**, 101–102.

Topp G., Davis J. and Annan A. 1980. Electromagnetic determination of soil water content: Measurement in coaxial transmission lines. *Water Resources Research* **16**, 574–582.

Vereecken H., Binley A.M., Cassiani G., Revil A. and Titov K. 2006. *Applied Hydrogeophysics*. Springer.

Vereecken H., Kemna A., Münch H.-M., Tillmann A. and Verweerd A. 2005. Aquifer characterization by geophysical methods. In: *Encyclopedia of Hydrological Sciences* (ed. M.G. Anderson), pp. 2265–2283. John Wiley and Sons.

Vereecken H., Yaramanci U. and Kemna A. 2002. Noninvasive methods in hydrology. *Journal of Hydrology* **267**.

Wagner K.W. 1924. Erklarung der Dielectrishen Nachwirkungsvorgange auf grund Maxwellscher vorstellungen. *Archiv Electrotechnik* **2**, 371–387.

West L.J., Handley K., Huang Y. and Pokar M. 2003. Radar frequency dielectric dispersion in sand and sandstone: Implications for determination of moisture content and clay content. *Water Resources Research* **39**, 1026. doi:10.1029/2001WR000923.

Wharton R.P., Hazen G.A., Rau R.N. and Best D.L. 1980. Electromagnetic propagation logging: Advances in technique and interpretation. SPE paper, No. 9267.

Woodside W. and Messmer J.H. 1961. Thermal conductivity of porous media. I. Unconsolidated sands. *Journal of Applied Physics* **32**, 1688–1699.

Wyllie M.R.J., Gregory A.R. and Gardner L.W. 1956. Elastic wave velocities in heterogeneous and porous media. *Geophysics* **21**, 41–70.

Zakri T., Laurent J.-P. and Vauclin M. 1998. Theoretical evidence for 'Lichtenecker's mixture formulae' based on effective medium theory. *Journal of Physics D: Applied Physics* **31**, 1589–1594.